A CFD – FEA CO-SIMULATION TO INVESTIGATE THE EFFECTS OF THERMAL BARRIER COATINGS ON GASOLINE COMPRESSION IGNITION COMBUSTION

Prakash Koirala

Abstract

Thermal barrier coatings (TBCs) have the potential to reduce heat transfer losses from engines and thereby improve engine efficiency. GCI combustion is a new, advanced combustion strategy that is both efficient and produces low emissions. In this study, we used a coating material called Gadolinium Zirconate (Gd-Zr) TBC on the piston of a GCI engine running at 1500rpm and at three different operating conditions of 6-bar, 10-bar, and 15-bar. The goal was to use modeling to determine how this coating affects the engine's performance. We found that the TBC made the engine's surface temperature swing more than 100K, and this helped reduce heat loss from the gas to the walls, making the engine more efficient. A coupled modeling of CFD and FEA to simultaneously analyze fluid flow and structural behaviors under various conditions was used until a quasi-steady state was achieved. This integrated approach allows for a comprehensive evaluation of both the thermal and mechanical performance of materials and components in a simulated environment, such as assessing the heat distribution within an engine coated with TBCs.

The computer simulations using CFD and FEA predicted that the TBC coating could improve efficiency by about 0.5 percentage points compared to an uncoated metal engine for all three operating conditions. However, when these TBCs were tested experimentally in real engines, a different trend emerged wherein there was an slight efficiency improvement at the low loads that matched the CFD-FEA results, but there was a slight efficiency penalty at the highest load, which did not agree with the CFD-FEA results. A possible reason for this difference is the theory of "convection vive", which is a phenomenon where combustion occurring in the near-wall thermal boundary layer causes the convective heat transfer coefficient to increase. Convection vive is not currently captured by CFD sub models, which might explain the discrepancy between the modeling results and the experiments. Future work could determine how convection vive, or any

other uncaptured physical phenomena, could be included in the computer predictions to improve their accuracy. A more advanced direct numerical simulation (DNS) study could help by effectively capturing the near-wall thermal conditions and combustion reactions.

Objectives of the current study

A coupled CFD-FEA methodology is developed that links a CFD model to FEA model of the piston within which several iterations is performed until a quasi-steady state converged solution was reached. The co-simulation framework is used to analyze thermal boundary conditions and predict efficiency gains.

The objectives of the study are summarized below:

- To develop and validate a co-simulation framework that integrates CFD and FEA for studying the impact of TBCs on GCI combustion.
- To investigate the effect of Gadolinium Zirconate (Gd-Zr) TBC on the temperature behavior of engine components, specifically focusing on the piston surface temperature swings during engine cycles.
- To assess the influence of TBCs on heat transfer losses and thermal efficiency within the GCI combustion environment under various operational pressures.
- To quantify the improvements in thermal efficiency due to TBC application through computational predictions and compare these with experimental results to evaluate the fidelity of the models.
- To identify and analyze the discrepancies between simulated predictions and actual experimental outcomes to enhance the understanding of TBC behavior in real-world engine conditions.
- To provide a foundation for future research directions, including the refinement of simulation models, exploration of different TBC materials, and assessment of TBCs in practical engine applications for sustainability and performance enhancement.

MODELING METHODOLOGY

3D CFD Computational Model

A 3D CFD model was created using CONVERGE 3-D CFD software. The model geometry was developed from Computer-Aided Design (CAD) models of relevant production engine parts provided by Aramco Services Company (ASC) in support of this study. Figure 1 shows the computational model developed for single cylinder, experimental engine. The simulation featured an injector positioned at the center, modeled accurately within CONVERGE Studio.

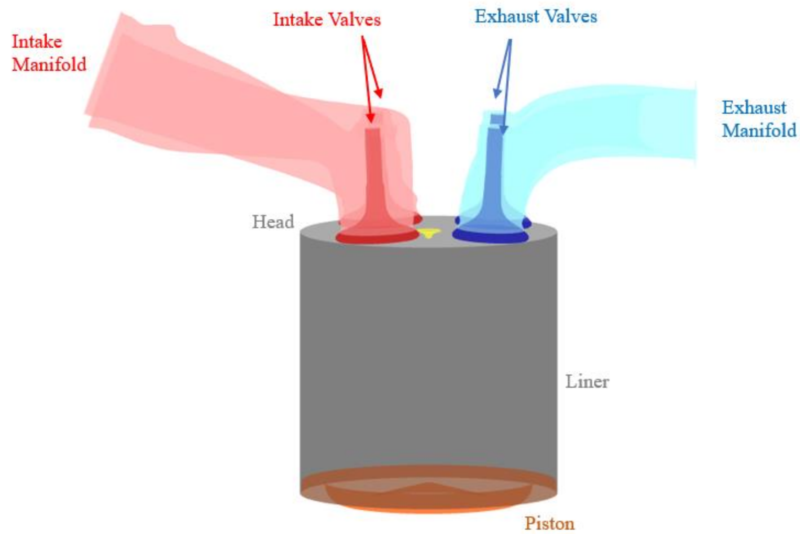

Figure 1: Computational model developed for single cylinder, experimental engine

Table 1 shows the engine specifications of single cylinder, experimental GDI engine.

Table 1: Engine specifications of single cylinder, experimental GDI engine

Bore	82mm
Stroke	80.1mm
Connecting Rod Length	152.4mm
Geometric Compression Ratio	15.6:1

Intake Valve Opening/ Closing	-360/-153 CAD aTDC
Exhaust Valve Opening/ Closing	127/358 CAD aTDC
Engine speed	1500 rpm

Table 2: Injector specifications

No. of nozzle holes	8
Nozzle diameter [µm]	110
Spray included Angle [°]	150
Spray Cone Angle [°]	17
Nozzle Discharge Coefficient [-]	0.79

3D FEA Model Framework

The FEA Model was developed using ABAQUS 2020 using the CAD model of the piston. The FEA modeling primarily involves simulating the heat transfer dynamics between the piston and the engine's combustion chamber.

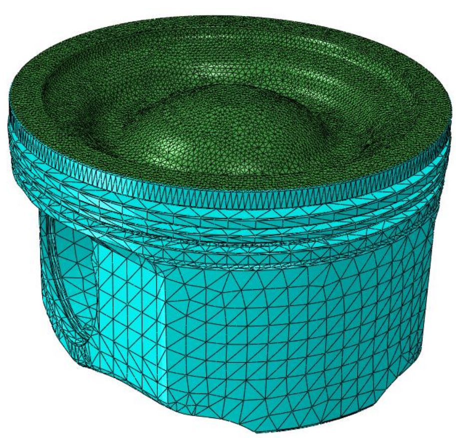

Figure 2: Geometry of piston with TBC layer coated on top (green)

Table 3 shows the material properties of the piston and TBC material.

Table 3: Piston and TBC material properties

Components	Piston	TBC
Density	5000 kg/m^3	5850 kg/m^3
Specific heat capacity	600 J/kg K	430 J/kg K
Thermal conductivity	42.5 W/m-K	0.74 W/m-K

RESULTS AND DISCUSSIONS

3D Computational Fluid Dynamics

The CAD parts of engine components were provided by Aramco Services Company (ASC) in support of this research work. At first, the metal baseline pistons were simulated and validated against the experimental data under 6-bar, 10-bar, and 15-bar operating conditions. The motoring data was validated followed by the firing data. For metal baseline, fixed embedding was not imposed on the piston surface. For coated case, a fixed embedding layer of about 1mm was imposed on the piston top surface to mimic the coating. Figure 3 shows the model validations for 6-bar operating conditions. The simulation has sufficient agreement with the experimental data to consider the model validated.

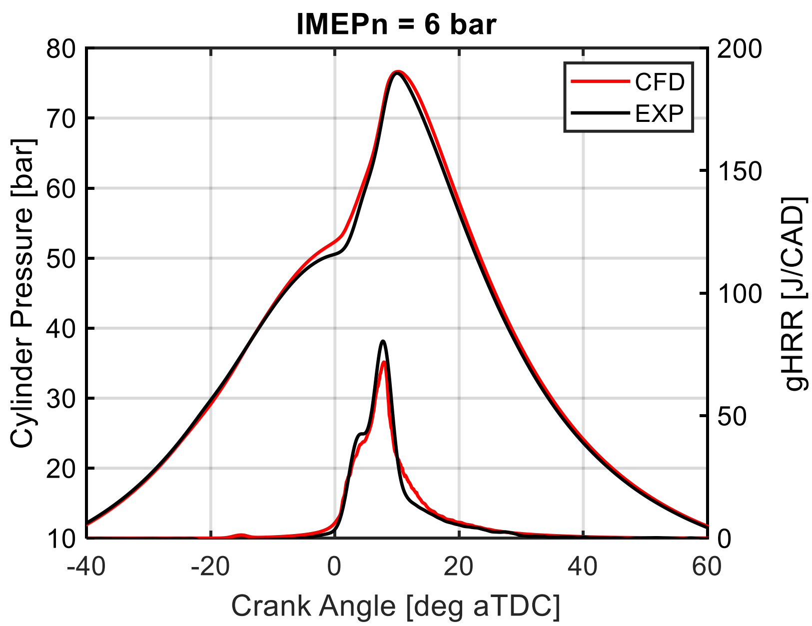

Figure 3: Cylinder pressure vs Gross Heat Release Rate (GHRR) for CFD (red) and Experiment (black) at 6 bar conditions

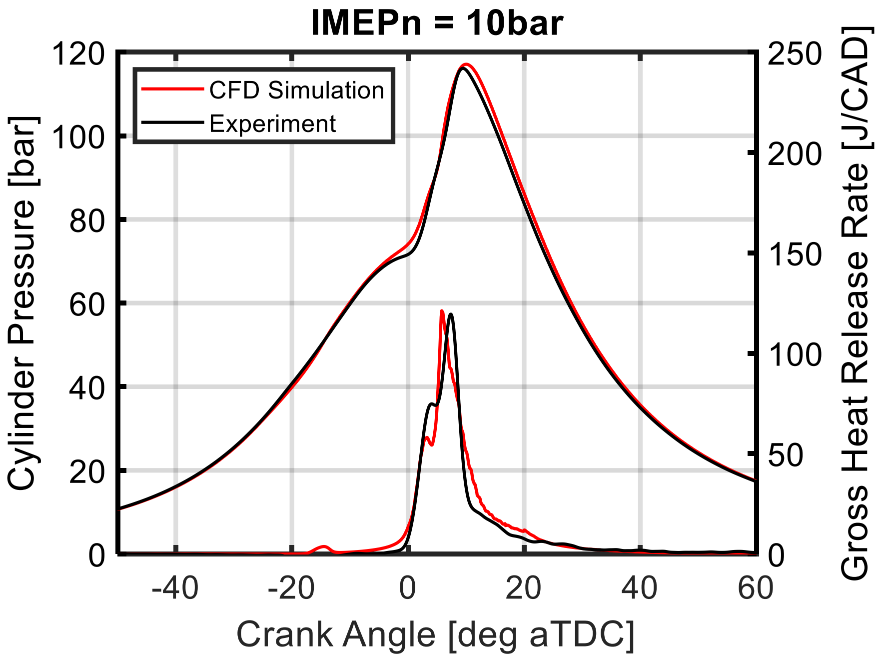

Figure 4: Cylinder pressure vs Gross Heat Release Rate (GHRR) for CFD (red) and Experiment (black) at 10 bar conditions

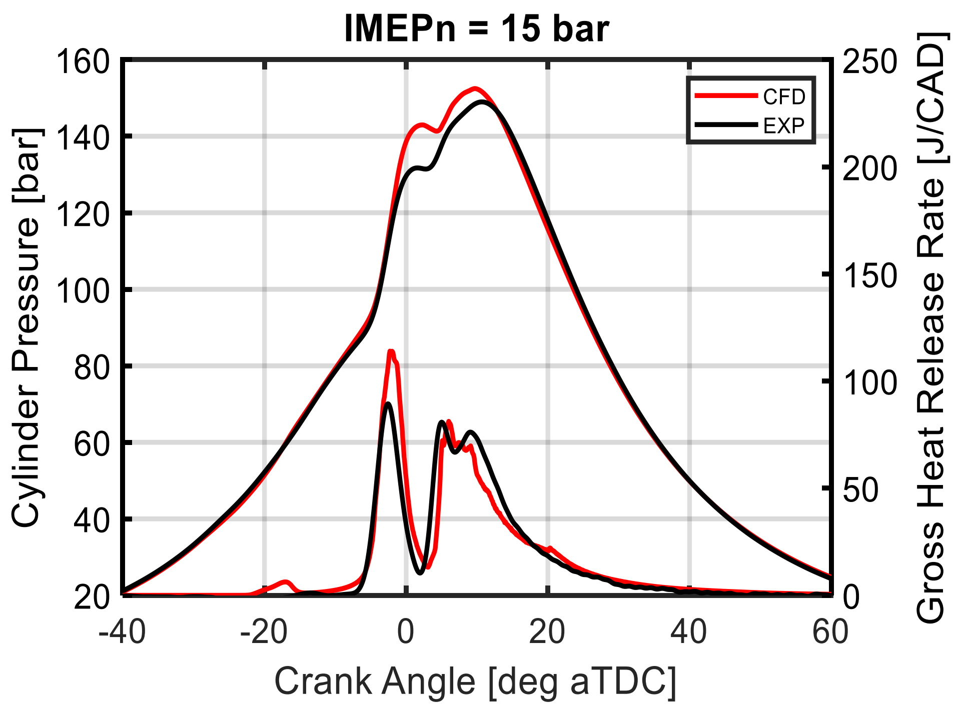

Figure 5: Cylinder pressure vs Gross Heat Release Rate (GHRR) for CFD (red) and Experiment (black) at 15 bar conditions

Additionally, a split fraction sweep was performed for the validation of CFD and the experimental traces. The experimental split fraction was 43% for the pilot injection and 57% for the main injection. The CFD model previously validated has the split fraction the same as the experiment. The sweeps were performed by increasing the main injection split fraction from 57% to 67%, from where 62% of the main injection and 38% of the pilot injection seem to agree reasonably well with the experiment.

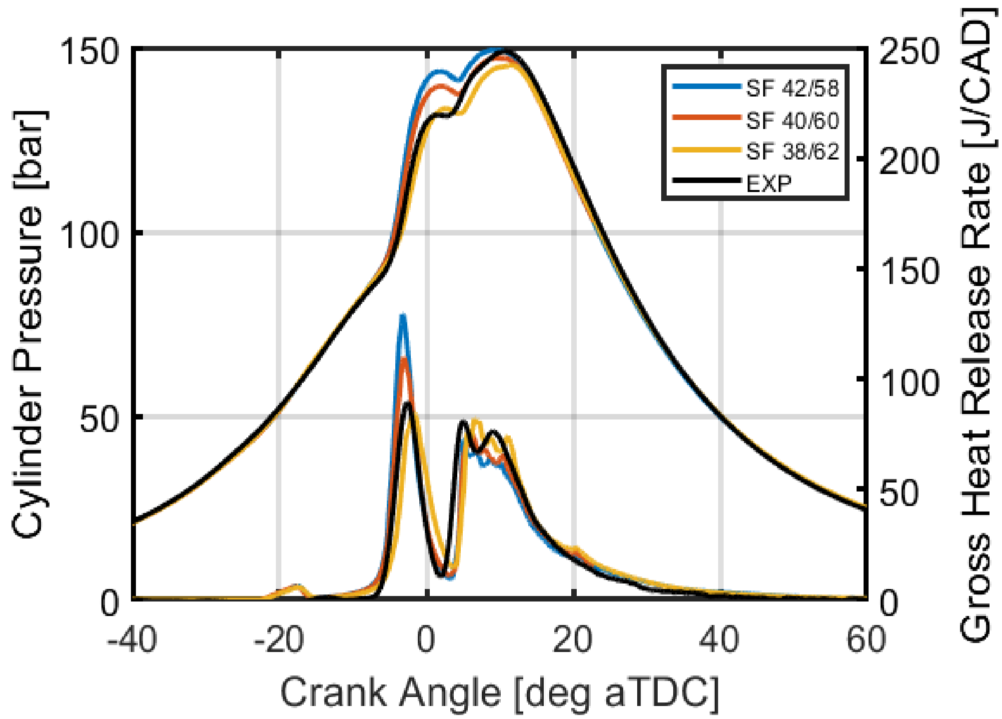

Figure 6: Cylinder pressure vs Gross Heat Release Rate (GHRR) for different split fractions (SF) with the experimental trace (black) at 15 bar conditions

3D Finite Element Analysis

The boundary conditions from 3D CFD output are imposed to FEA model of the piston. At first, the metal baseline is simulated. Figure 7 shows the coated piston surface temperature and nodal temperatures for 6 bar conditions.

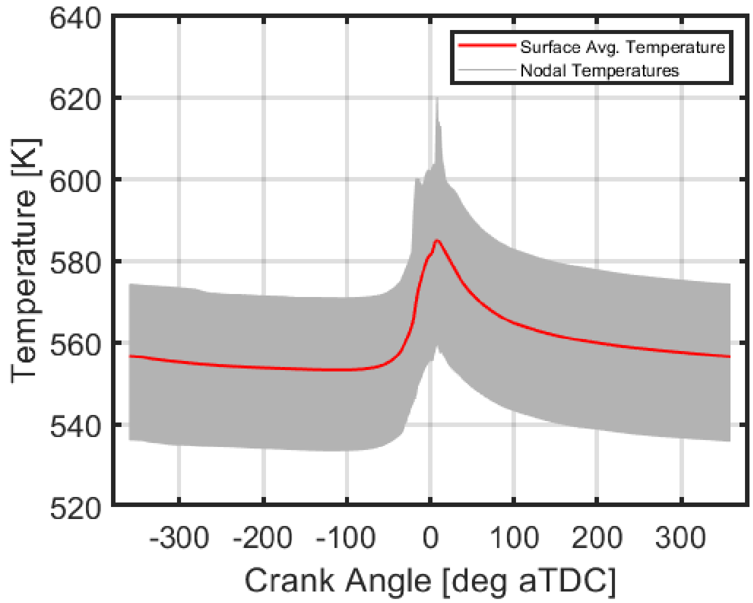

Figure 7: Surface average temperature (red) and Nodal Temperatures (grey) variation for TBC coated piston at 6 bar conditions

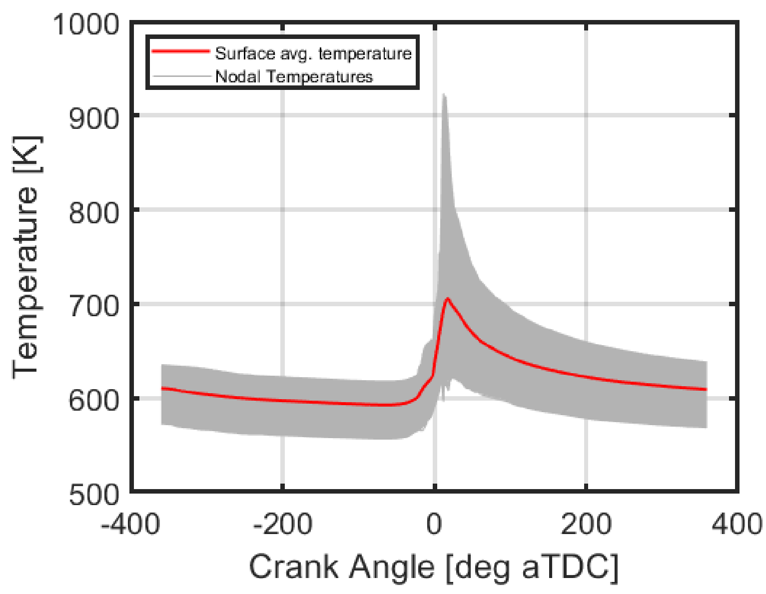

Figure 8: Surface average temperature (red) and Nodal Temperatures (grey) variation for TBC coated piston at 10 bar conditions

The larger temperature variation reflects a more vigorous combustion process, which in turn generates more heat. At this intermediate pressure condition, the TBC is still performing its insulative role, but the increased heat flux from the combustion gases to the piston surface results in higher surface temperatures.

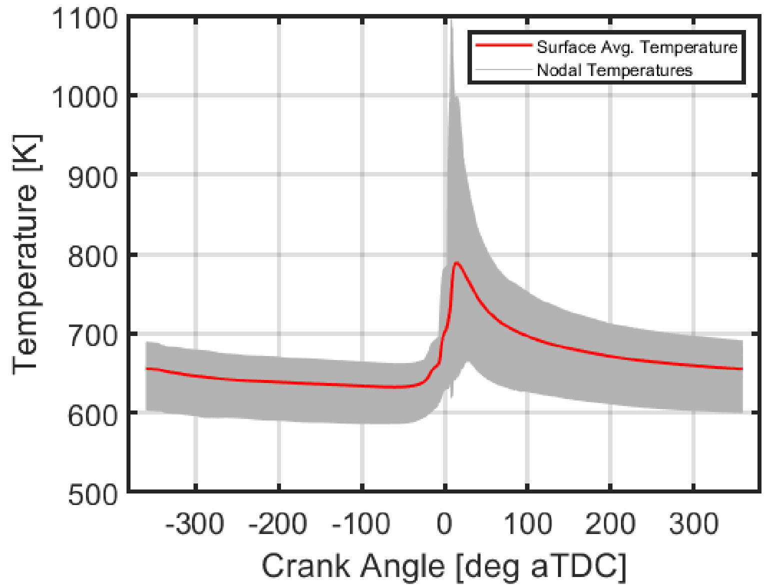

Figure 9: Surface average temperature (red) and Nodal Temperatures (grey) variation for TBC coated piston at 15 bar conditions

3D CFD-FEA Co-simulation

The 3D CFD model was first ran with constant piston wall temperature of 450K which is the CFD Baseline case. After running the first FEA iteration with piston thermal boundary conditions from CFD, transient wall temperature profile was generated from FEA which was used for the next iteration of CFD-FEA Co-simulation.

The figures below show plots of cylinder pressure versus gross heat release rate for different CFD iterations during co-simulation at 6 bar, 10 bar, and 15 bar conditions. These plots are essential for validating the CFD model's ability to simulate the real-world behaviors observed in engine testing (EXP). The data from these simulations helps in understanding the combustion dynamics within the engine cylinder for each operating condition.

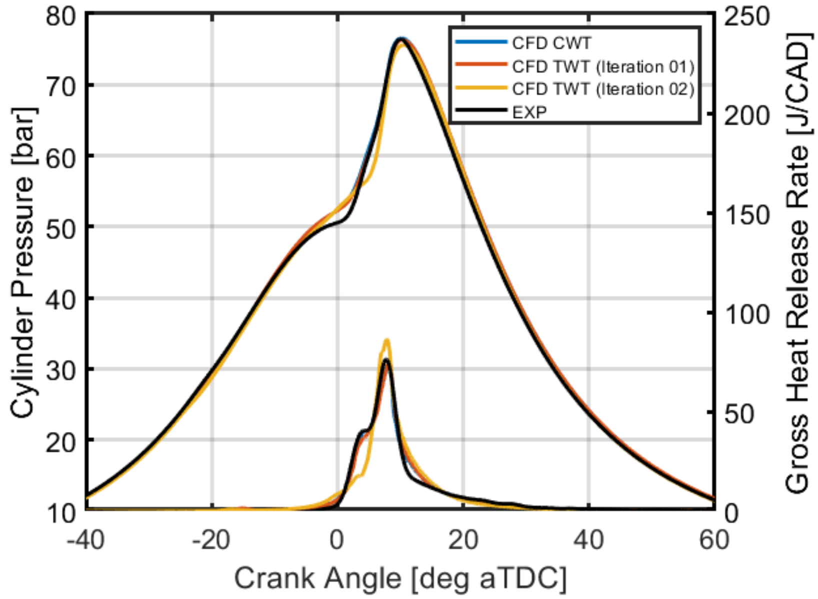

Figure 10: Cylinder pressure vs Gross Heat Release Rate from CFD output during the co-simulation iterations at 6 bar conditions

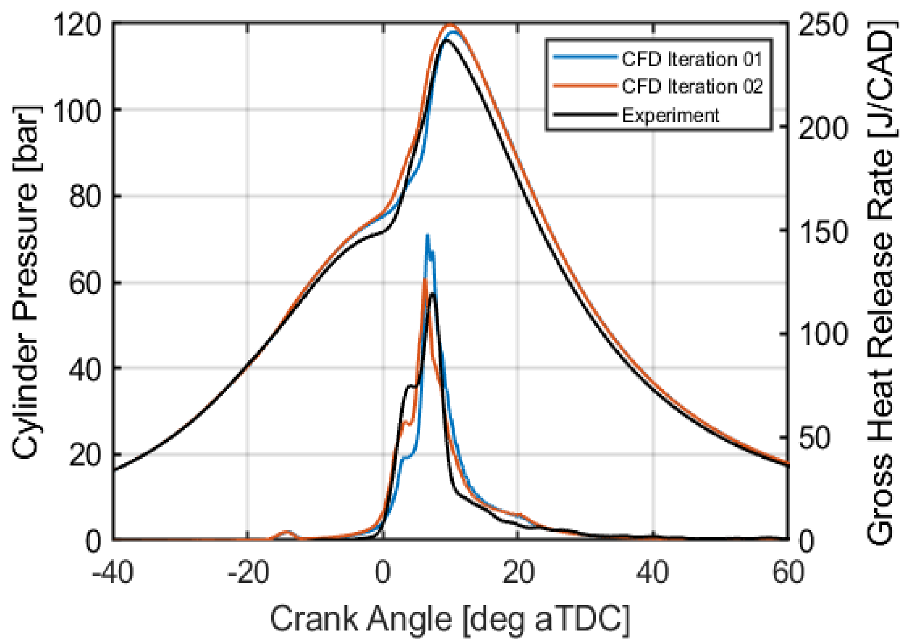

Figure 11: Cylinder pressure vs Gross Heat Release Rate from CFD output during the co-simulation iterations at 10 bar conditions

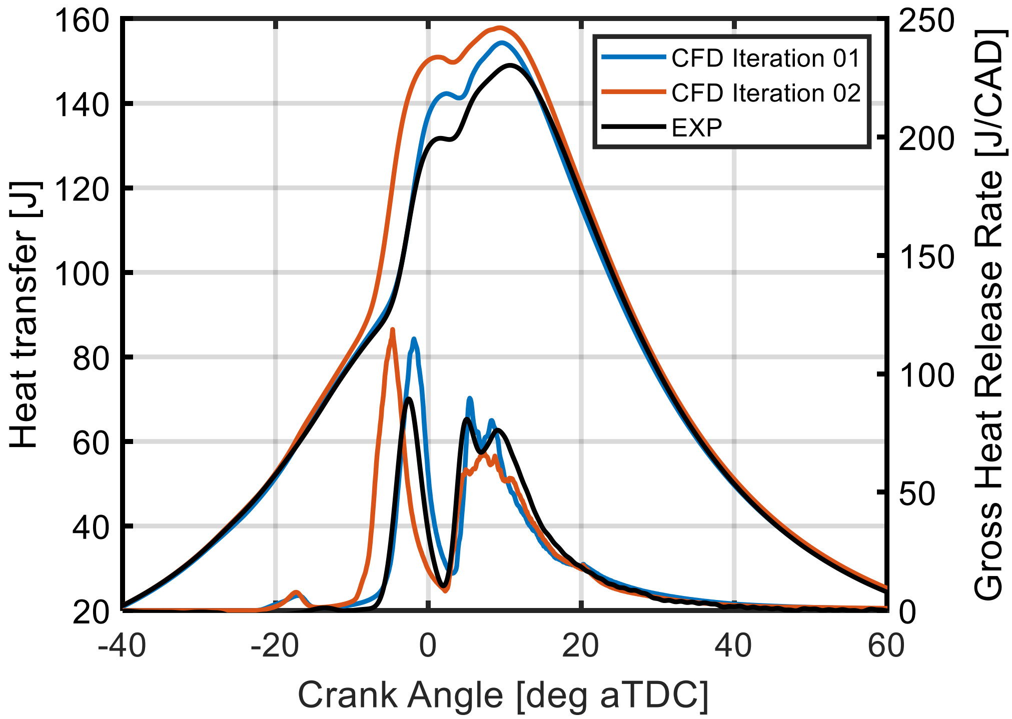

Figure 12: Cylinder pressure vs Gross Heat Release Rate from CFD output during the co-simulation iterations at 15 bar conditions

During the co-simulation routine, the heat transfer data from CONVERGE, which shows how heat moves on the piston surface over time, was sorted using a MATLAB script. Figure 13 shows 3D CFD-FEA Co-simulation Framework developed for the current study. This script organized the data based on where it was on the piston and what the temperature was. Then, a new time step was created using a Python script in Abaqus, a software used for simulating engineering problems. This new time step used the heat transfer data to make sure the heat flow was accurate. After the simulation, the results, which showed the temperature of the piston surface at different times and places, were saved in a text file. This file was then used in the next iteration of the simulation in CONVERGE.

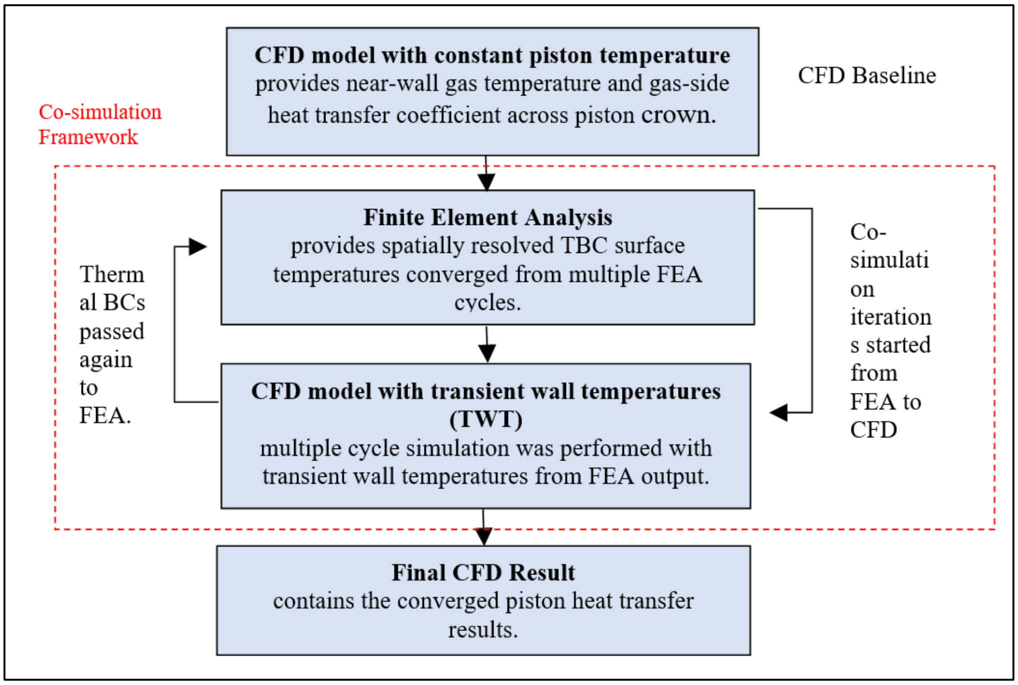

Figure 13: 3D CFD-FEA Co-simulation Framework.

The co-simulation was performed for a 250-micron thick TBC layer, where the temperature swing phenomenon depends on the difference between gas and the wall that reduces heat transfer through the piston. Since the change in cycle averaged uncoated piston temperature was less than 2K, a quasi-steady solution can be assumed. Figure 14 shows the surface average temperature variations during an engine cycle for the uncoated and coated pistons along with constant wall temperatures used as initialization for metal and TBC cases.

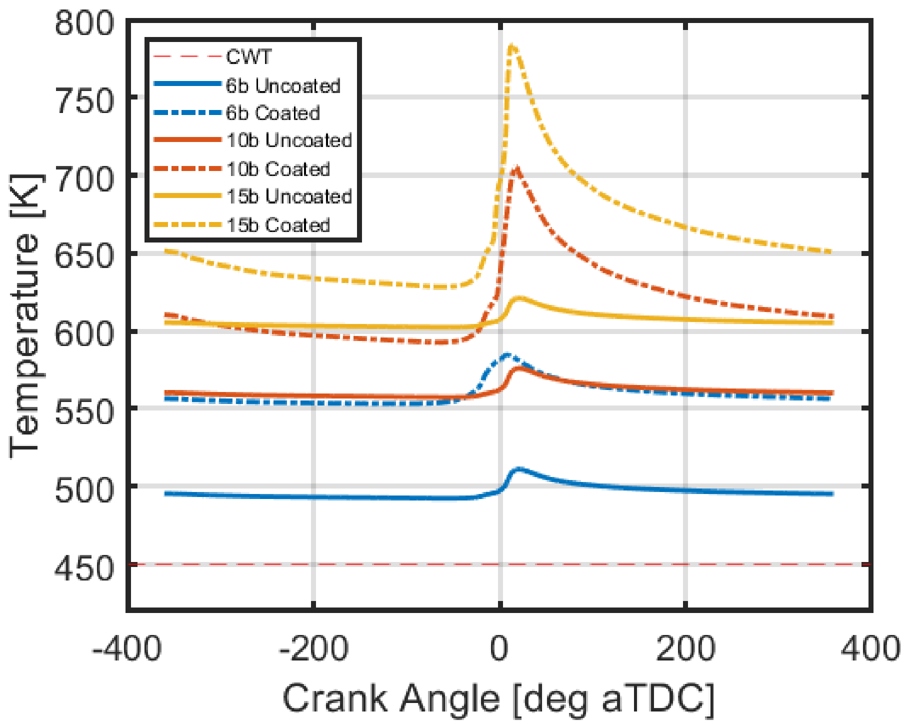

Figure 14: Comparison of piston surface averaged temperature for uncoated (solid) and coated (dashed) cases for the final iteration of FEA with transient wall temperatures along with constant wall temperature (red-dashed)

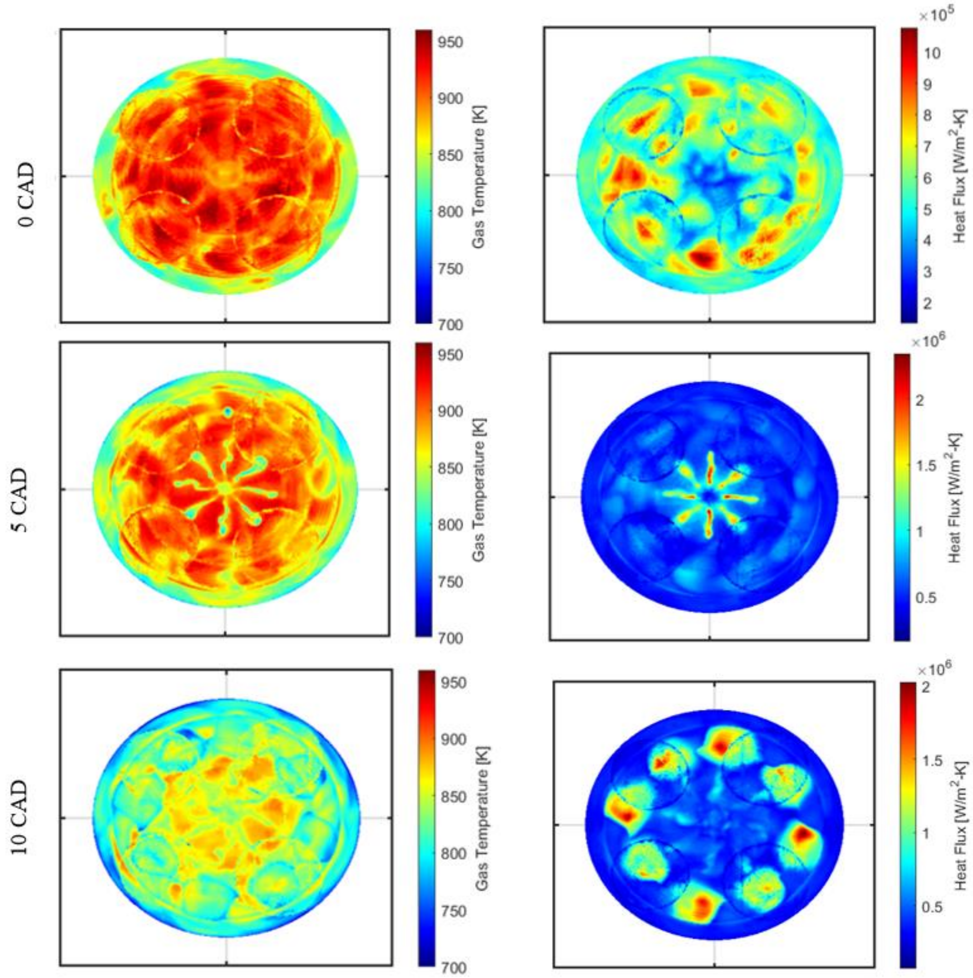

Figure 15: Near-wall gas temperature (left) and heat flux (right) at 0 CAD, 5 CAD and 10 CAD aTDC for 6 bar conditions

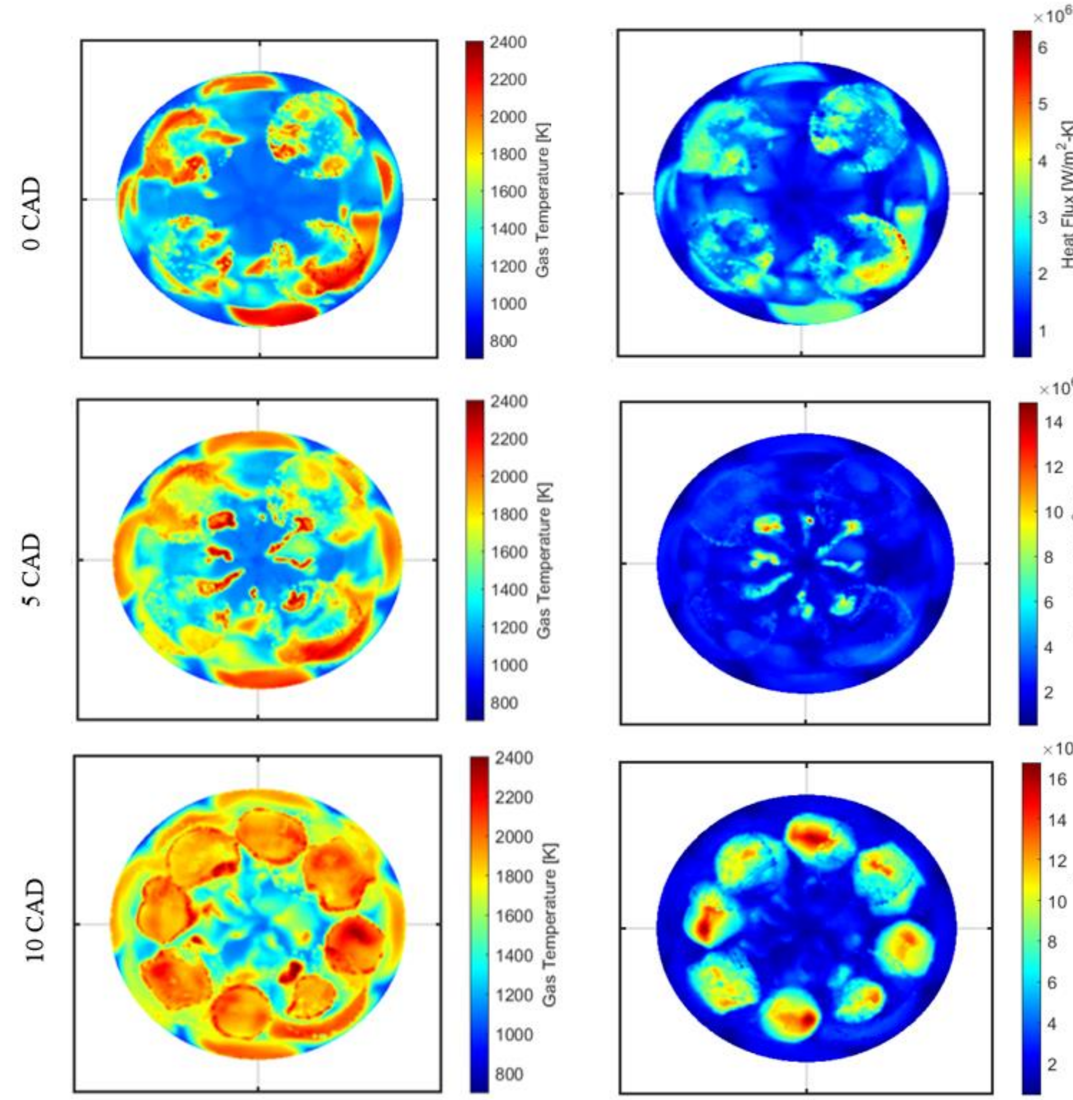

Figure 16: Near-wall gas temperature (left) and heat flux (right) at 0 CAD, 5 CAD and 10 CAD aTDC for 10 bar conditions

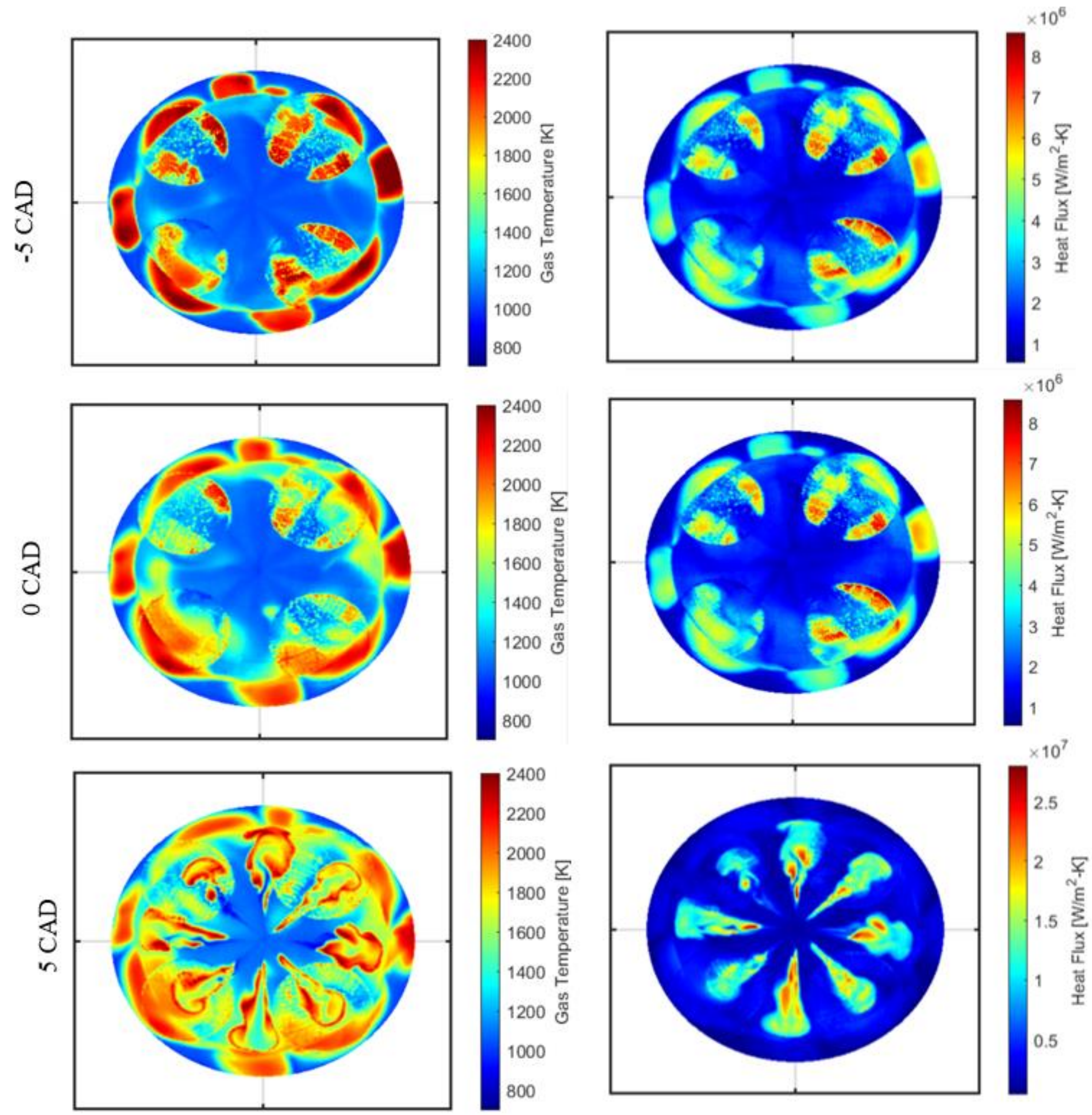

Figure 17: Near-wall gas temperature (left) and heat flux (right) at 0 CAD, 5 CAD and 10 CAD aTDC for 15 bar conditions

The results for the comparison of several performance parameters for 6-bar, 10-bar and 15-bar conditions are provided in Table 4, Table 5, and Table 6, respectively. The combustion was phased a bit earlier with the addition of TBC, during the co-simulation iteration. Therefore, a slight reduction in intake temperature was done to match the combustion phasing. At the 6-bar condition, both uncoated and coated pistons show higher net indicated mean effective pressure (IMEP) compared to experimental results, with the coated piston slightly outperforming the uncoated.

Table 4: Performance parameters comparisons for uncoated and coated piston with experimental results at a net IMEP of 6 bar

Parameters	**Uncoated Metal Piston**	**TBC-Coated Piston**	**Experiment**
Net IMEP [bar]	6.28	6.31	5.85±0.04
IVC Pressure [bar]	1.41	1.41	1.42±0.11
IVC Temperature [K]	421	420	426±10
Peak Pressure [bar]	76.35	76.3	76.41±0.10
MPRR [bar/CAD]	5.44	5.21	5.92±1.01
Net fuel efficiency [%]	42.12	42.28	44.35±0.11
Net thermal efficiency [%]	42.35	42.79	44.7±0.15
Gross fuel efficiency [%]	42.7	43	45.1±0.11
Combustion efficiency [%]	99.67	98.80	99.29±0.1
CA50 [CAD aTDC]	7.9	8	8.2±0.1
Exhaust Temperature [K]	658.27	661.51	648.54±10

Table 5: Performance parameters comparisons for uncoated and coated piston with experimental results at net IMEP 10 bar

Parameters	**Uncoated Metal Piston**	**TBC-Coated Piston**	**Experiment**
Net IMEP [bar]	10.74	10.78	9.84±0.04
IVC Pressure [bar]	1.82	1.81	1.83±0.11
IVC Temperature [K]	383	381	370±10
Peak Pressure [bar]	118.44	119.72	116.11±0.10
MPRR [bar/CAD]	10.86	9.8	10.34±1.01
Net fuel efficiency [%]	44.82	45.31	43.68±0.11
Net thermal efficiency [%]	45.05	45.5	44.31±0.15
Gross fuel efficiency [%]	45.33	45.82	45.65±0.11
Combustion efficiency [%]	99.48	99.69	98.66±0.1
CA50 [CAD aTDC]	7.3	7	7.5±0.1
Exhaust Temperature [K]	682.92	697.25	662.89±10

Table 6: Performance parameters comparisons for uncoated and coated piston with experimental results at net IMEP 15 bar

Parameters	Uncoated Metal Piston	TBC-Coated Piston	Experiment
Net IMEP [bar]	15.30	15.51	14.73±0.04
IVC Pressure [bar]	2.39	2.39	2.37±0.11
IVC Temperature [K]	381	384	370±10
Peak Pressure [bar]	154.31	159.27	148.97±0.10
MPRR [bar/CAD]	13.47	21.52	11.80±1.01
Net fuel efficiency [%]	43.15	43.71	44.35±0.11
Net thermal efficiency [%]	43.37	43.84	44.70±0.15
Gross fuel efficiency [%]	43.4	43.96	45.65±0.11
Combustion efficiency [%]	99.47	99.72	99.52±0.1
CA50 [CAD aTDC]	6.8	7	7.9±0.1
Exhaust Temperature [K]	714.23	735.59	697.25±10

The thermal efficiency for 10 bar and 15 bar conditions was predicted to be higher than the experiment for the TBC-coated piston but for 6 bar conditions, it was lower. On comparing the cumulative heat transfer through the piston, it was found that about 17% reduction of heat loss due to the temperature swing phenomenon of TBCs for 10-bar conditions. As compared to conventional SI and diesel combustion studies, we have seen a reduction of roughly about 7% and 10%, respectively [33, 34]. However, the 17% reduction in heat transfer only translated to a 0.5 percentage point improvement in efficiency. Figure 19 shows cumulative heat transfer through uncoated and coated pistons for 6-bar conditions. It depicts how TBC affect the heat transfer characteristics of pistons in GCI combustion mode. For the 6-bar condition, the graph indicates that the heat transfer for the coated piston closely follows that of the uncoated one until the combustion phase.

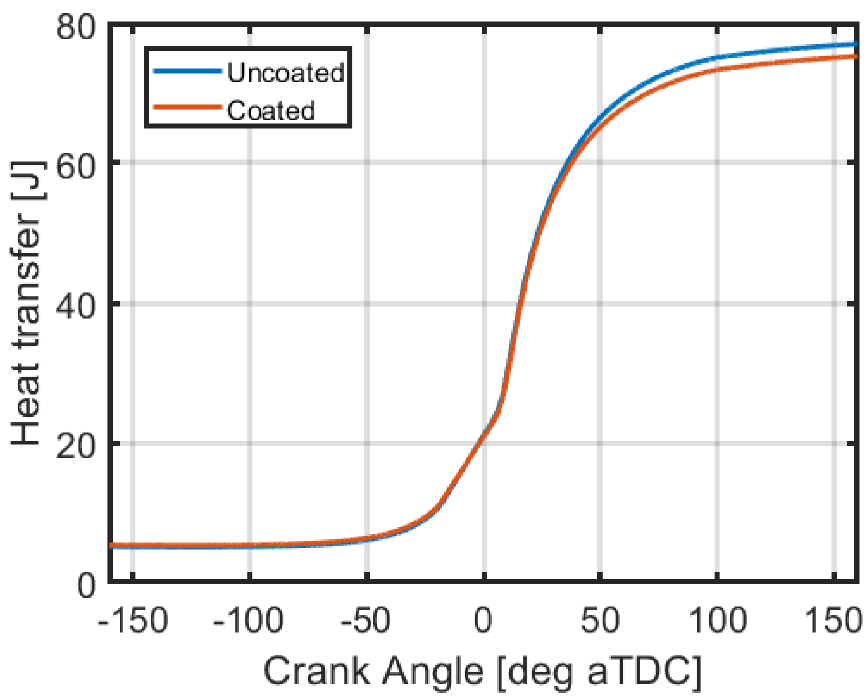

Figure 18: Cumulative heat transfer through piston for uncoated (blue) and coated (red) at 6-bar conditions

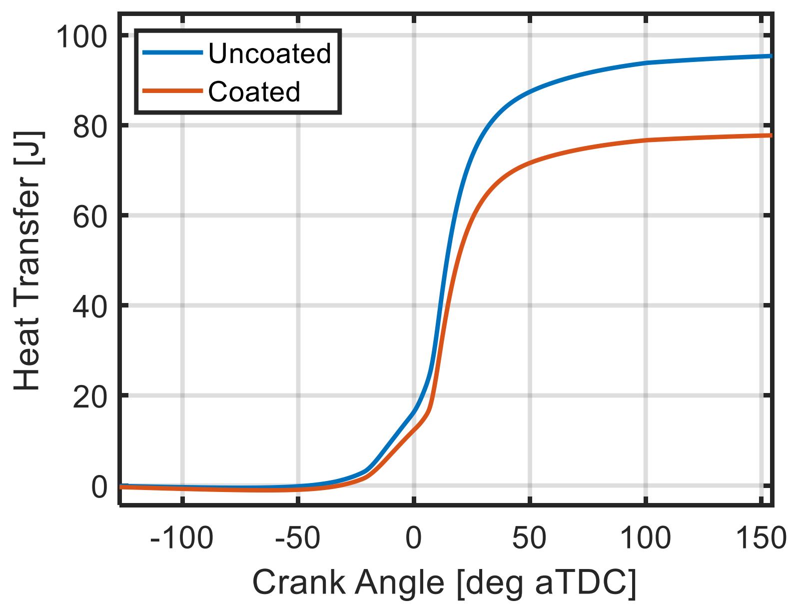

Figure 19: Cumulative heat transfer through piston for uncoated (blue) and coated (red) at 10-bar conditions

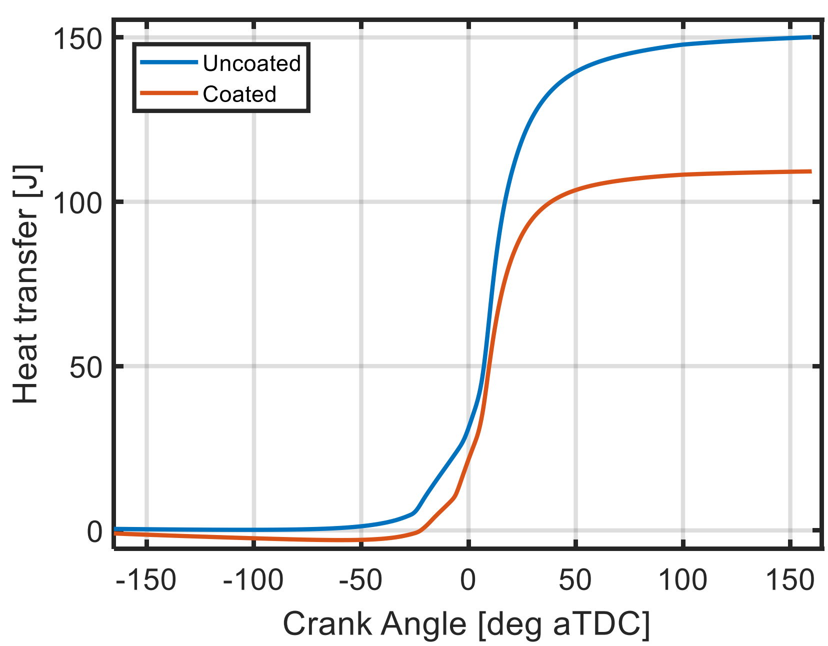

Figure 20: Cumulative heat transfer through piston for uncoated (blue) and coated (red) at 15-bar conditions

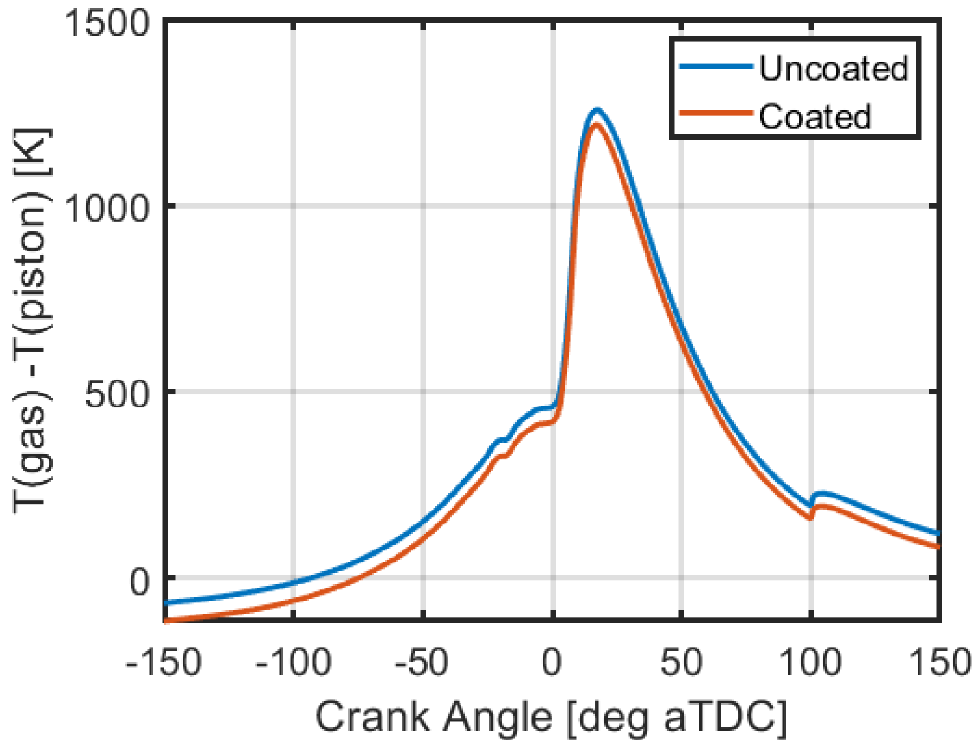

Figure 21: Gas temperature minus piston temperature for uncoated (blue) and coated (red) at 6-bar conditions

This suggests that the surface of the coated piston is hotter compared to the uncoated one during the combustion phase. Since heat transfer depends on the temperature difference between the gas and the piston, a higher piston surface temperature in the coated piston could lead to reduced heat transfer to the piston during this phase. It appears that the TBC's insulating effect becomes less pronounced at lower pressure conditions, as evidenced by the smaller temperature difference.

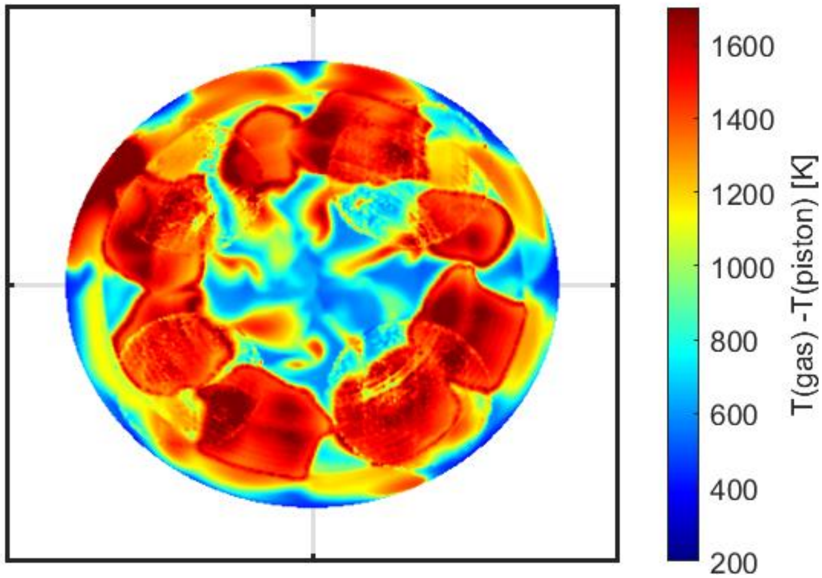

Figure 22: Gas temperature minus piston temperature for uncoated piston on the piston surface at 15 CAD aTDC for 6 bar conditions

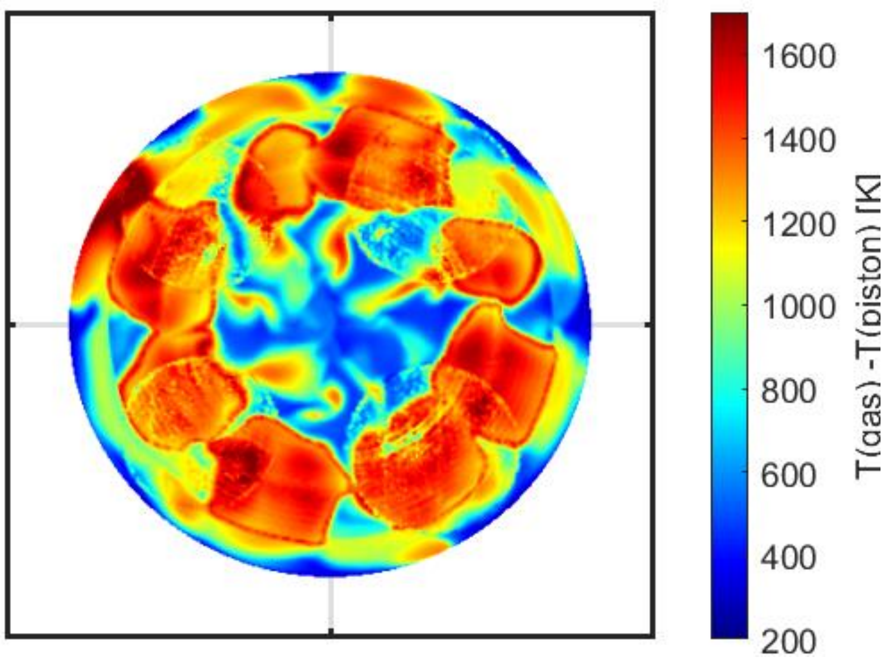

Figure 23: Gas temperature minus piston temperature for coated piston on the piston surface at 15 CAD aTDC for 6 bar conditions

Figure 23 illustrates the difference in temperature between the gas and the piston surface over the course of the engine cycle, comparing uncoated and TBC-coated pistons at 10 bar conditions.

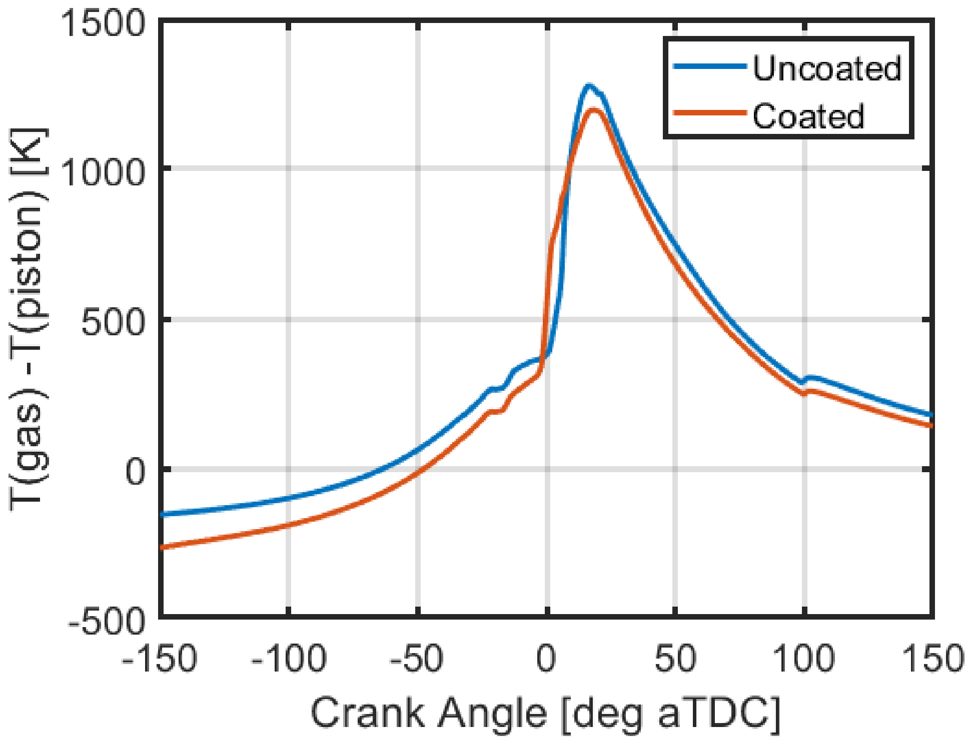

Figure 24: Gas temperature minus piston temperature for uncoated (blue) and coated (red) at 10-bar conditions

For the 10-bar condition, the trend continues, but the difference in temperature between the gas and the piston surface increases as the load increases.

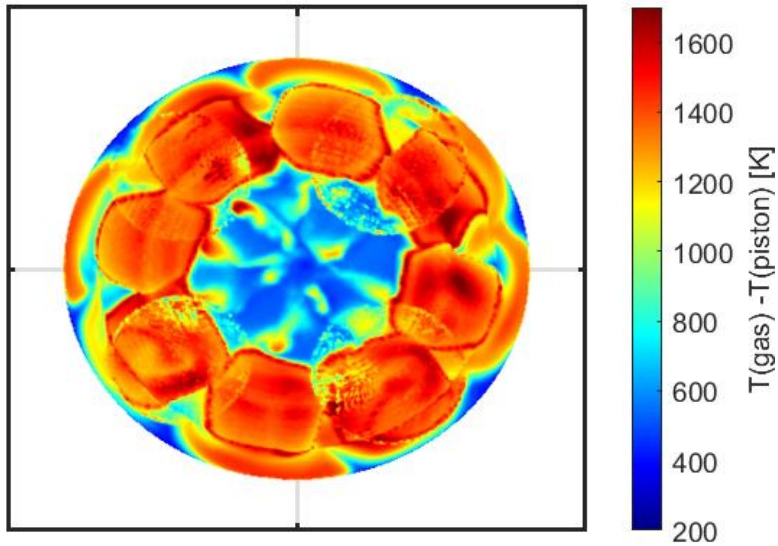

Figure 25: Gas temperature minus piston temperature for uncoated piston on the piston surface at 15 CAD aTDC for 10 bar conditions

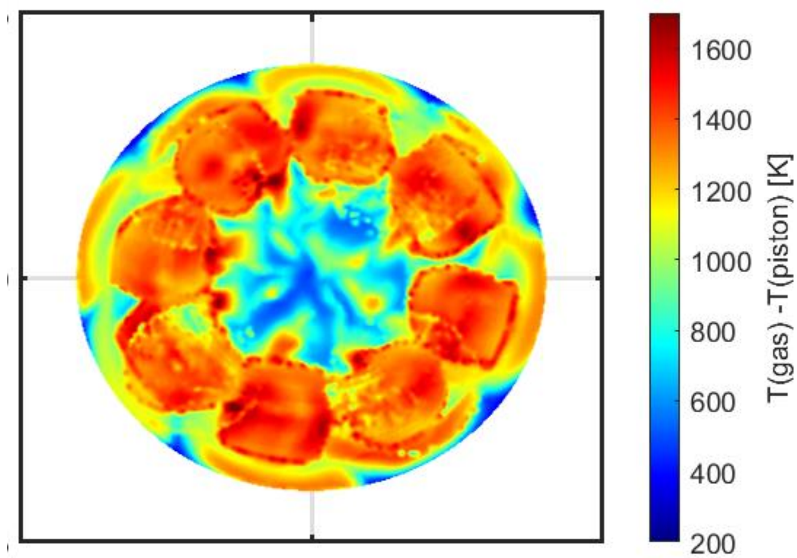

Figure 26: Gas temperature minus piston temperature for coated piston on the piston surface at 15 CAD aTDC for 10 bar conditions

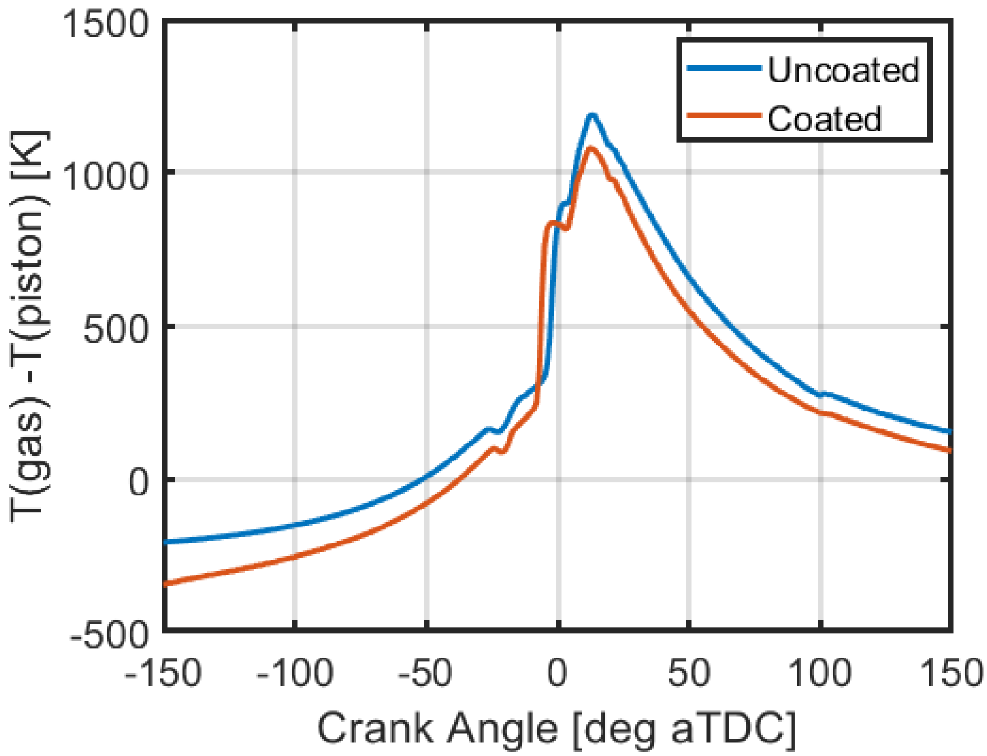

Figure 27: Gas temperature minus piston temperature for uncoated (blue) and coated (red) at 15-bar conditions

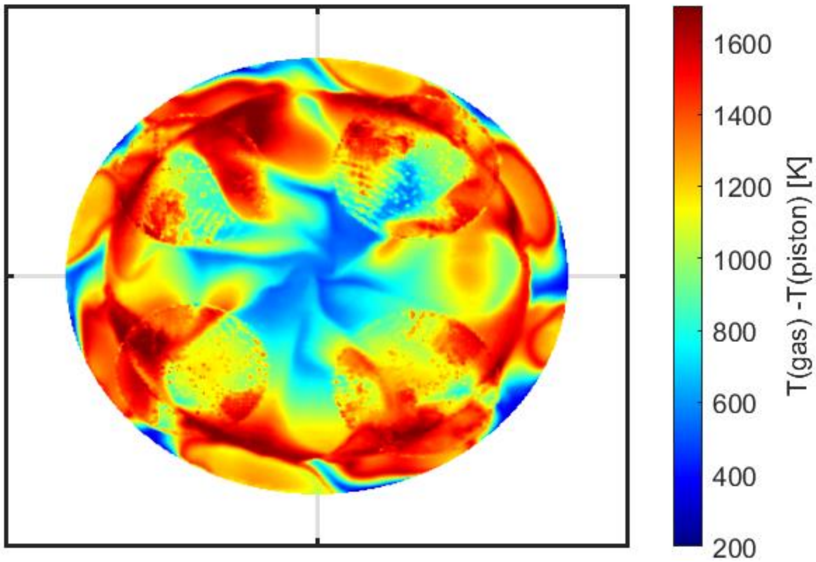

Figure 28: Gas temperature minus piston temperature for uncoated piston on the piston surface at 15CAD aTDC for 15 bar conditions

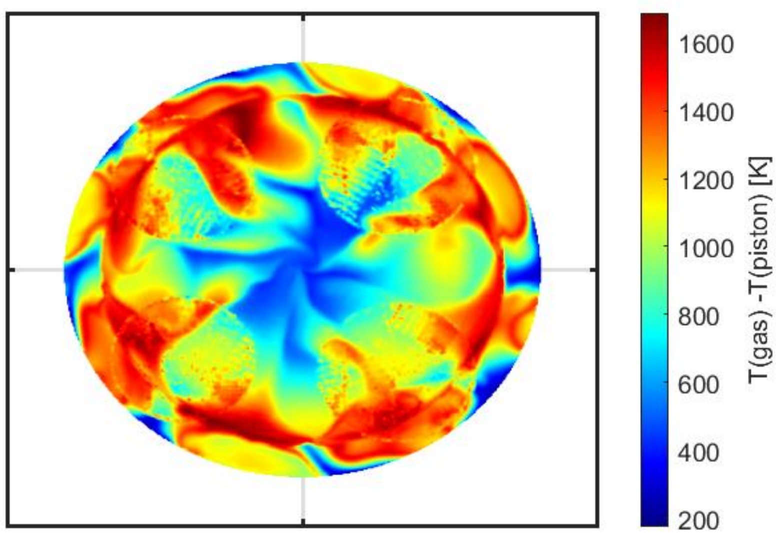

Figure 29: Gas temperature minus piston temperature for coated piston on the piston surface at 15CAD aTDC for 15 bar conditions

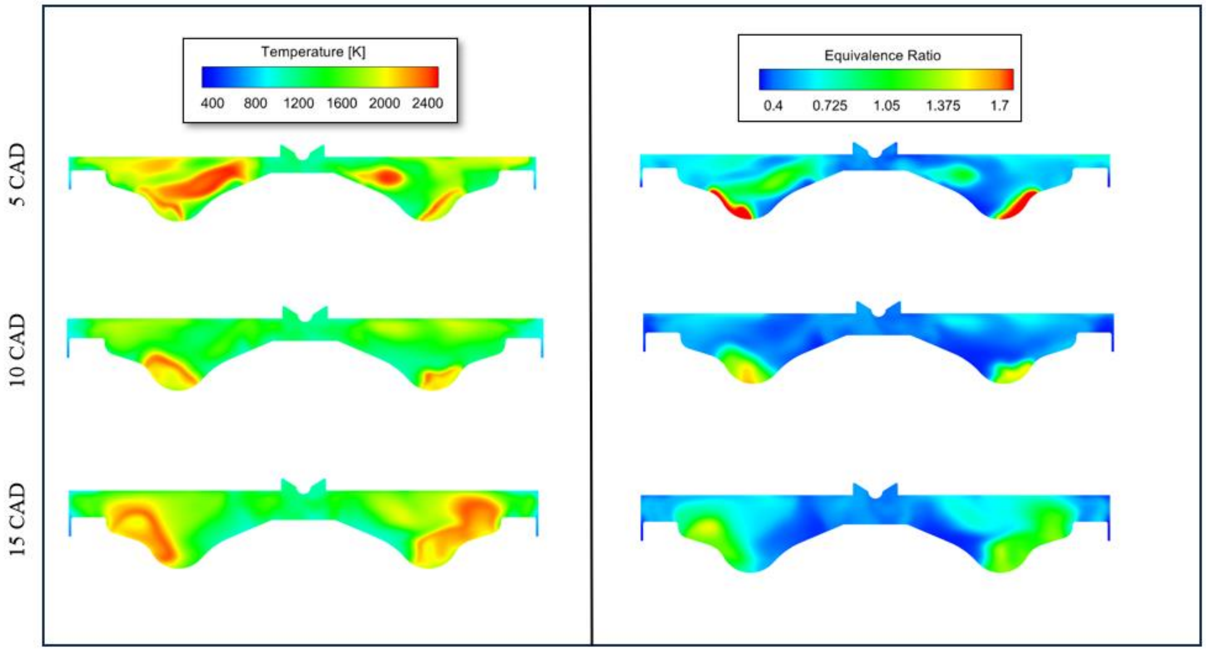

Figure 30: Cut-plane visualizations for temperature (left) and equivalence ratio (right) distributions at 5, 10, and 15 CAD aTDC for coated piston at 6-bar conditions

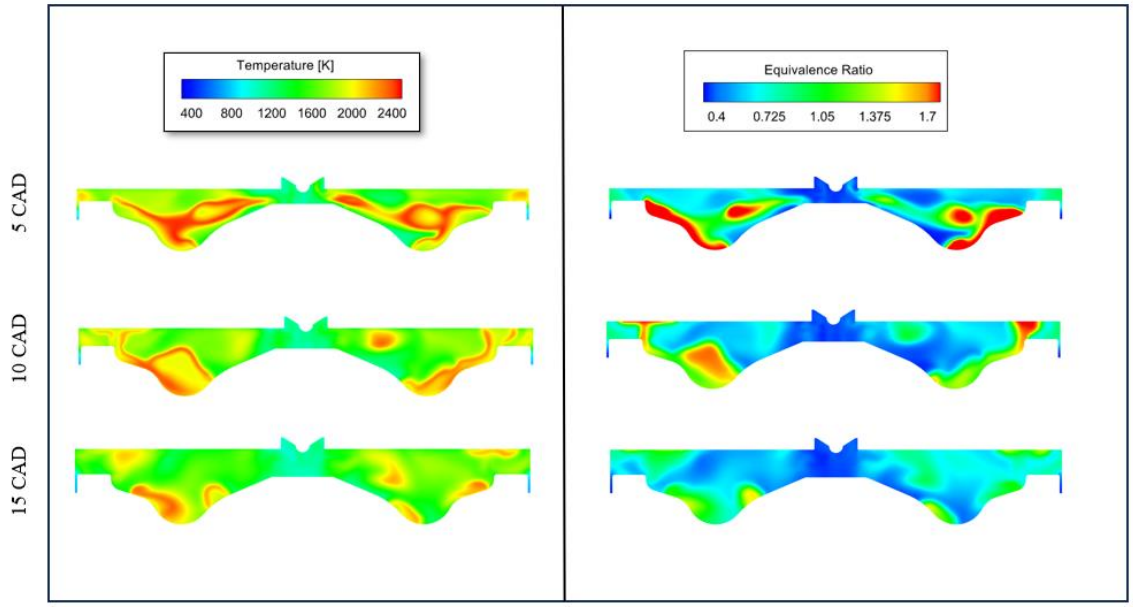

Figure 31: Cut-plane visualizations for temperature (left) and equivalence ratio (right) distributions at 5, 10, and 15 CAD aTDC for coated piston at 10-bar conditions

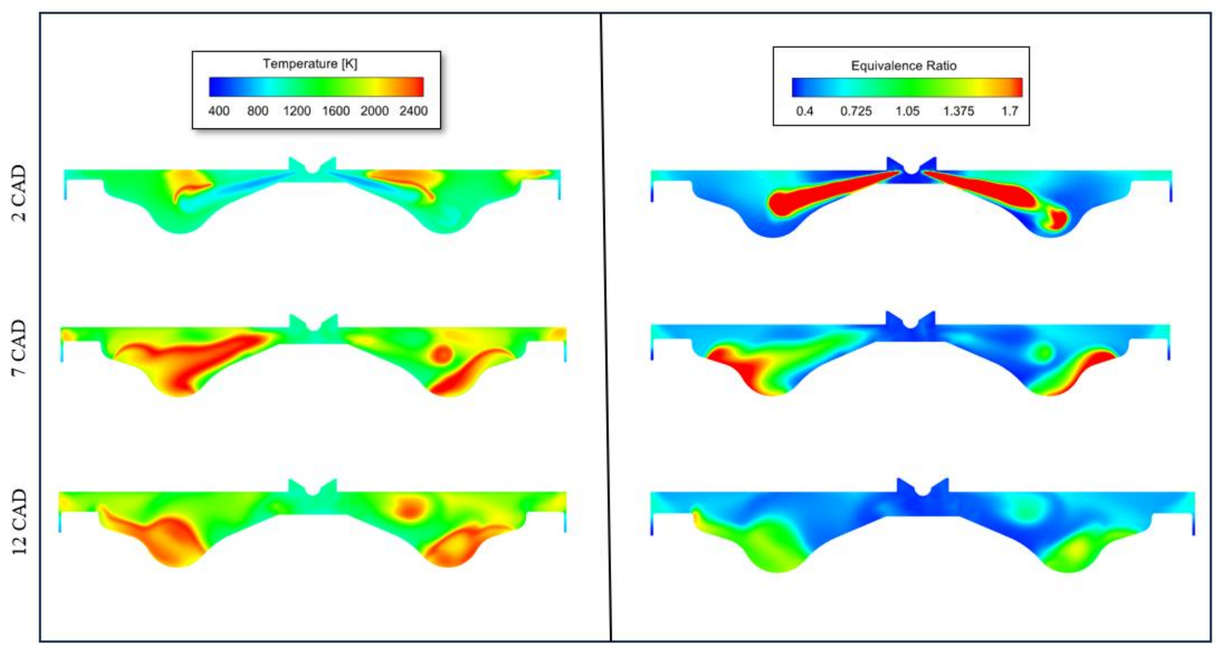

Figure 32: Cut-plane visualizations for temperature (left) and equivalence ratio (right) distributions at 2, 7, and 12 CAD aTDC for coated piston at 15-bar conditions

In the visualizations, especially at the higher 10 bar condition, there are noticeable hot zones where the TBC will be most stressed. The performance of the TBCs in these areas is crucial for engine longevity and efficiency. If the TBCs deteriorate, the thermal management capabilities of the engine could be compromised, leading to reduced efficiency and potential engine damage due to overheating.

CONCLUSIONS AND RECOMMENDATIONS FOR FUTURE WORK

The study is on the co-simulation of CFD and FEA, which has led to a distinct understanding of TBCs' impact on GCI combustion mode. The computer models CFD and FEA were used to study how a coating gadolinium zirconate TBC affects heat transfer and efficiency in GCI combustion. These models were linked together so they could work together to understand what happens inside the engine piston. It took three iterations to get the models to agree on how the piston behaves. In the end, the surface of the TBC-coated piston got hotter than a regular metal piston, reaching 930K with a swing of 100K, compared to 619K for the metal piston for medium load operating conditions. We also adjusted the timing of combustion to match the real-world conditions better. The TBC reduced heat loss by 5% for 6 bar conditions, and about 17% for 10-bar conditions, and according to our models, it should improve efficiency by 0.5 percentage points. Similarly, for the 15-bar coated case, the heat transfer loss was found to reduce about 36%. However, when these coating were experimentally tested in real engines, there was a slight efficiency improvement at low loads, but a slight efficiency penalty at the higher load operating conditions of 15 bar. It is found that this trend is due to increase in near wall heat transfer coefficient caused by "convection vive" affecting the near-wall thermal boundary layer. At a load of 10 bar, the efficiency was the same with or without the coating.

- The application of Gadolinium Zirconate (GdZr) as a TBC is shown to significantly influence the temperature regulation within the combustion chamber. It manages to contain the surface temperature fluctuations, which in turn impacts the thermal efficiency positively by mitigating heat loss through the piston walls.
- The simulations predicted a modest but notable improvement in thermal efficiency attributable to the TBC application. However, this theoretical efficiency gain was not seen in experimental outcomes, indicating that real-world complexities might not be fully captured by the simulation models.
- The inconsistency between the predicted and actual efficiency improvements highlights the complex nature of heat transfer in GCI and suggests a potential gap in the simulation's ability to capture all relevant heat transfer mechanisms.

- There is a clear indication from the simulation results that TBCs have the potential to reduce heat transfer through the piston by a considerable margin, demonstrating the role TBCs could play in thermal management and performance optimization in GCI.

There are several paths for further research that could expand the current understanding of TBCs.

- To improve the match between simulated and actual engine behavior, a more extensive validation of the CFD and FEA models is recommended. This could involve comparing simulation results with experimental data across a wider range of operating scenarios, engine speeds, and loads.
- The study suggests the necessity for more sophisticated simulation methodologies that can more accurately model the distinct heat transfer phenomena, especially the convective heat transfer that seems to play a critical role in engine wall temperature dynamics.
- A closer look into the turbulence models and fuel injection simulations could help in enhancing the predictive accuracy of the models. Since these factors have a significant influence on the combustion process, refining these models could lead to better optimization of engine performance.
- There is room for investigation into different TBC materials and configurations. These studies could provide insights into the thermal and mechanical properties that best suit the high-load and high-temperature conditions of GCI.
- Given the high temperatures and pressures involved in GCI, a comprehensive analysis of the thermo-mechanical stresses experienced by TBCs could provide valuable information on their durability and operational longevity.
- Applying the findings to real-world GCI and assessing the impact on actual vehicle performance would be the ultimate test of the TBCs' viability. These studies should focus on long-term efficiency, emissions profiles, and durability under typical driving conditions.

*****